Journal of Organometallic Chemistry 696 (2011) 4104–4111

Contents lists available at ScienceDirect

Journal of Organometallic Chemistry

journal homepage: www.elsevier.com/locate/jorganchem

Organomagnesium clusters: Structure, stability, and bonding in archetypal models

J. Oscar C. Jiménez-Halla [a], F. Matthias Bickelhaupt [b,*], Miquel Solà [c,**]

[a] Department of Organic Chemistry, Arrhenius Laboratory, Stockholm University, SE-10691 Stockholm, Sweden
[b] Department of Theoretical Chemistry and Amsterdam Center for Multiscale Modeling, Scheikundig Laboratorium der Vrije Universiteit, De Boelelaan 1083, NL-1081 HV Amsterdam, The Netherlands
[c] Institut de Química Computacional and Departament de Química, Universitat de Girona, Campus Montilivi, E-17071 Girona, Catalonia, Spain

ARTICLE INFO

Article history:
Received 18 May 2011
Received in revised form
7 June 2011
Accepted 10 June 2011

Keywords:
Bond theory
Density functional calculations
Grignard reagents
Magnesium
Polar bonds

ABSTRACT

We have studied the molecular structure and the nature of the chemical bond in the monomers and tetramers of the Grignard reagent CH_3MgCl as well as MgX_2 (X = H, Cl, and CH_3) at the BP86/TZ2P level of theory. For the tetramers, we discuss the stability of three possible molecular structures of C_{2h}, D_{2h}, and T_d symmetry. The most stable structure for $(MgCl_2)_4$ is D_{2h}, the one for $(MgH_2)_4$ is C_{2h}, and that of $(CH_3MgCl)_4$ is T_d. The latter is 38 kcal/mol more stable with chlorines in bridge positions and methyl groups coordinated to a Mg vertex than *vice versa*. We find through a quantitative energy decomposition analysis (EDA) that the tetramerization energy is predominantly composed of electrostatic attraction ΔV_{elstat} (60% of all bonding terms $\Delta V_{elstat} + \Delta E_{oi}$) although the orbital interaction ΔE_{oi} also provides an important contribution (40%).

1. Introduction

The synthesis of diethylzinc by Frankland in the mid nineteenth century [1] and the remarkable work of Grignard on organomagnesium reagents at the beginning of the last century [2] paved the way for the development of modern organometallic chemistry. Organometallic compounds have provided many synthetic solutions. In particular, they have been used in the synthesis of fine chemicals such as additives, plasticizers, drugs, or other high-value items. Examples of versatile organometallic systems in organic synthesis are the polar organometallic compounds having metal–carbon bonds, such as organolithium, organoberyllium, organomagnesium, and organozinc compounds [3]. Grignard reagents [4,5], RMgX (R = alkyl or aryl; X = halogen), are especially relevant since they can be used, amongst others, to introduce functional groups or to form new carbon–carbon bonds in cross-coupling reactions (eq (1)).

$$R{-}MgX + R'{-}X' \rightarrow R{-}R' + MgXX' \qquad (1)$$

In concentrated solution and/or weakly basic solvents, organomagnesium compounds have a certain tendency toward association and exchange substitution that yields a complex mixture with various species in equilibrium [6,7]. Thus, in solution, Grignard reagents RMgX are in equilibrium with R_2Mg and MgX_2 (the so-called Schlenk equilibrium [8]) and at the same time these species (RMgX, R_2Mg, and MgX_2) exist in equilibrium as a collection of monomers, dimers, trimers, tetramers, and higher oligomers, the proportion of each one depending on the nature of R, X, concentration, solvent, and temperature [5]. In the case of $MgCl_2$, computational studies indicate that association could even lead to beautiful structures such as sheets and nanotubes [9]. In most cases, in these molecular structures the tetracoordination of magnesium is retained via formation of electron deficient 3c–2e bonds between magnesium and two ligands R (or in some cases 3c–4e bonds) leading to a formal octet around magnesium [6].

One might expect that organomagnesium compounds, being less polar than organolithium compounds, have a lower tendency to form aggregates [10]. Yet, such organomagnesium oligomers do exist in solution. These aggregates are characterized by their floppiness [11,12] and, therefore, several structures of higher oligomers can coexist in solution [13,14]. Thus, it is clear that these organomagnesium systems possess a beautiful and complex structural chemistry that is fascinating on its own. At the same

* Corresponding author. Fax: +31 20 59 87 629.
** Corresponding author. Fax: +34 972 41 83 56.
E-mail addresses: F.M.Bickelhaupt@vu.nl (F.M. Bickelhaupt), miquel.sola@udg.edu (M. Solà).

0022-328X/$ – see front matter © 2011 Elsevier B.V. All rights reserved.
doi:10.1016/j.jorganchem.2011.06.014

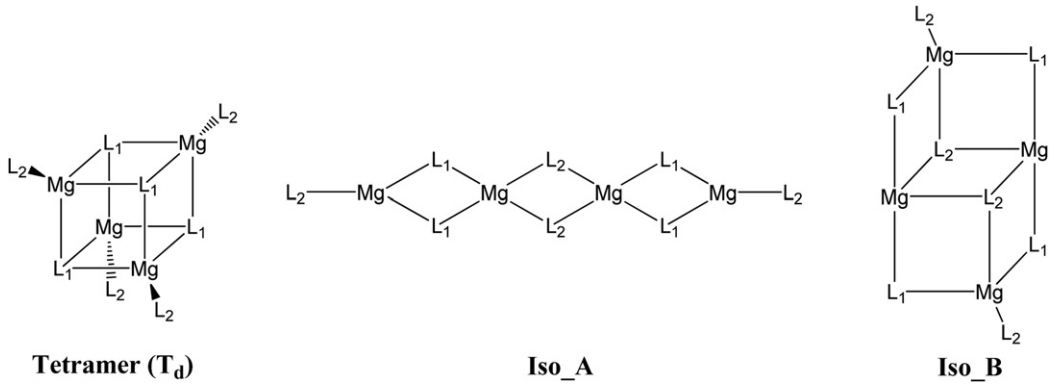

Scheme 1. Structures analyzed for L_1–Mg–L_2 tetramers.

time, understanding this complexity is important for designing synthetic pathways involving Grignard reactions.

Despite the extensive use of Grignard reagents in organic synthesis, details concerning their molecular structure, modes of formation and aggregation, and reaction mechanisms are still topics of current research. In the present work, we analyze the tetramerization process in the CH_3MgCl Grignard reagent and in MgX_2 (X = H, Cl, and CH_3) species with two main goals: first, to determine which is the most stable molecular structure for the different tetramers among structures of T_d, C_{2h}, and D_{2h} symmetry (see Scheme 1) and, second, for the cubic T_d tetramers, to analyze the bonding between the monomers through an energy decomposition analysis (EDA) and compare the results with those obtained earlier (at the same level) for the corresponding organolithium tetramers.

In previous studies, we have analyzed the structure and bonding (*e.g.*, through EDA) in various alkalimetal–element aggregates: $[M(CH_3)]_n$ [15,16], $[MF]_n$ [17], $[MH]_n$ [18], and $[MCl]_n$ [19] (M = Li, Na, K and Rb; and n = 1, 4). The tetrahedral structure of $[Mg^{2+}(CH_3Cl)^{2-}]_4$ and $[Mg^{2+}(X_2)^{2-}]_4$ is analogous to that of $[M^+X^-]_4$ (M = Li, Na, K, and Rb; X = H, Cl, and CH_3) which is well-known in organolithium chemistry. In a purely ionic model the cubic T_d arrangement is indeed the most stable one since the dipole–dipole interactions between monomers are maximized [20]. Moreover, the existence of heterometallic organomagnesium complexes with alkalimetals is indicative for similarities in the bonding situation [6]. Our EDA analyses allow us to compare the nature of the bonding in corresponding organomagnesium and organoalkalimetal compounds. Finally, MgH_2 has been investigated in the quest for efficient hydrogen storage materials [21]. Understanding the bonding between Mg and H_2 in aggregates can help to improve the processes of hydrogen uptake and release.

2. Theoretical methods

2.1. General procedure

All density functional theory (DFT) calculations were performed with the Amsterdam density functional (ADF) program [22,23]. The molecular orbitals (MOs) were expanded in a large uncontracted set of Slater type orbitals (STOs) of triple-ζ quality for all atoms and two sets of polarization functions were included (2*p* and 3*d* on H; 3*d* and 4*f* on C, Cl, and Mg) [24]. Moreover, an extra set of *p* functions has been added to the basis set of Mg (3*p*). The 1*s* core electrons of carbon and the 1*s*2*s*2*p* core shells of magnesium and chlorine were treated by the frozen core approximation [23] as it was shown to have a negligible effect on the obtained geometries [25]. An auxiliary set of *s*, *p*, *d*, *f*, and *g* STOs was used to fit the molecular density and to represent the Coulomb and exchange potentials accurately for each SCF cycle [26]. Energies and gradients were computed using the local density approximation (Slater exchange and VWN correlation [27]) with non-local corrections for exchange (Becke88) [28] and correlation (Perdew86) [29] included self-consistently (*i.e.*, the BP86 functional). Relativistic effects were not included since they are very small in bond distances and frequencies of species such as $MgBr_2$ [30]. Our BP86/TZ2P approach, in particular the TZ2P basis which contains relatively diffused STOs, has been previously shown to yield accurate structures and bond energies for organoalkalimetal clusters RM corresponding to the present organomagnesium clusters RMgR′ (R, R′ = CH_3, Cl, H) [15,31].

Analytical Hessians were computed to confirm the nature of the located stationary points. Bond enthalpies and Gibbs energies at 298.15 K and 1 atm (ΔH_{298} and ΔG_{298}) were calculated from electronic bond energies (ΔE) and frequency computations using standard statistical-mechanics relationships for an ideal gas [32]. Structures that we report have been verified to be (local) energy minima through vibrational analyses. In two cases, structures **Iso_3A** of Mg_4Me_8 (*i*12, *i*43, *i*45 cm^{-1}) and **Iso_4A** of $Mg_4Cl_4Me_4$ (*i*32, *i*32 cm^{-1}), we find very low imaginary frequencies which however correspond to the nearly-free methyl-group rotation.

Macroscopic solvent effects in a tetrahydrofuran (THF) solvent were additionally taken into account in some calculations using the COSMO model [33]. In this latter case, we have carried out a reoptimization of the species studied in the solution. The electron density distribution was analyzed using the Voronoi deformation density (VDD) method [31,34] and the Hirshfeld scheme [35] for computing atomic charges.

2.2. Bond energy decomposition

The overall tetramerization energy ($\Delta E = E([L_1MgL_2]_4) - 4E([L_1MgL_2])$; L_1 is the ligand in the bridge of the tetramer, see Scheme 1) is made up of two major components (eq (2)):

$$\Delta E = \Delta E_{prep} + \Delta E_{int} \quad (2)$$

In this formula, the preparation energy ΔE_{prep} is the amount of energy required to deform the separate monomers from their equilibrium structure to the geometry that they acquire in the tetramer. The interaction energy ΔE_{int} corresponds to the actual energy change when the prepared monomers are combined to form the overall molecule. It is analyzed for our model systems in the framework of the Kohn–Sham MO model using a Morokuma-type decomposition of the bonding energy into electrostatic

interaction, exchange repulsion (or Pauli repulsion), and (attractive) orbital interactions (eq (3)) [36].

$$\Delta E_{\text{int}} = \Delta V_{\text{elstat}} + \Delta E_{\text{Pauli}} + \Delta E_{\text{oi}} \quad (3)$$

The term ΔV_{elstat} corresponds to the classical electrostatic interaction between the unperturbed charge distributions of the prepared (*i.e.*, deformed) monomers and is usually attractive. The Pauli repulsion ΔE_{Pauli} comprises the destabilizing interactions between occupied orbitals. It arises as the energy change associated with going from the superposition of the unperturbed electron densities of the four monomers to the wavefunction $\Psi^0 = N\,A\,[\Psi_{L_1MgL_2}\Psi_{L_1MgL_2}\Psi_{L_1MgL_2}\Psi_{L_1MgL_2}]$, that properly obeys the Pauli principle through explicit antisymmetrization (A operator) and renormalization (N constant) of the product of fragment wavefunctions. It comprises the four-electron destabilizing interactions between occupied MOs and is responsible for any steric repulsion. The orbital interaction ΔE_{oi} is the change in energy from Ψ^0 to the final, fully converged wavefunction Ψ_{SCF} of the system. In any MO model, and therefore also in Kohn–Sham theory, the orbital interactions account for charge transfer (*i.e.*, donor–acceptor interactions between occupied orbitals on one fragment with unoccupied orbitals of the other, including the HOMO–LUMO interactions) and polarization (empty–occupied orbital mixing on one fragment due to the presence of another fragment).

3. Results and discussion

3.1. Monomers

The computed BP86/TZ2P geometries are shown in Fig. 1. All studied monomers are linear. It is well-known that magnesium dihalides are linear although this is not the case for all alkaline earth dihalides [12,30,37]. Our BP86/TZ2P distances are quite close to the experimental ones for MgH_2 (1.69582(4) obtained with microwave spectroscopy [38,39]), $MgCl_2$ (2.162 ± 0.005 Å [40] and 2.1856 ± 0.0114 Å [41] both obtained by electron diffraction). Unfortunately, for $Mg(CH_3)_2$ only the data for the Mg–C distance in the polymeric solid is available (2.24 Å [42]) and this value is not comparable with the gas-phase Mg–C bond length. Related compounds such as dineopentylmagnesium, Np_2Mg, have a Mg–C bond distance of 2.12 Å determined in gas-phase by neutron diffraction [43], which is close to our optimized value of 2.11 Å for $Mg(CH_3)_2$. This value is in the range of 2.12–2.18 Å found experimentally for Mg–C single-bond distances [10,44]. Finally, there is no experimental data on the molecular structure of CH_3MgCl [6]. Our BP86/TZ2P bond distances in Fig. 1 are also not far from the previously computed MP2/6-31G(d) values [45,46] of $d_{\text{Mg–H}}$ = 1.722 Å in MgH_2 (1.6957 Å with the MRCI/CBS method [39]), $d_{\text{Mg–Cl}}$ = 2.182 Å in $MgCl_2$ (2.181 Å at the MP2/6-311G(d) level [13]), $d_{\text{Mg–Cl}}$ = 2.207 Å in CH_3MgCl, $d_{\text{Mg–C}}$ = 2.104 Å in $Mg(CH_3)_2$, and $d_{\text{Mg–C}}$ = 2.082 Å in CH_3MgCl, differences being less than few hundredths of an Å. In addition, they are almost identical to previously reported BP86/TZ2P results [47]. The Mg–X distance in MgX_2 increases from 1.71 to 2.11 to 2.18 Å along X = H, CH_3, and Cl. Interestingly, the Mg–C distance decreases from 2.11 to 2.08 Å and the Mg–Cl increases from 2.18 to 2.21 Å when going from dimethylmagnesium and magnesium chloride, respectively, to methylmagnesium chloride. This is likely the result of the CH_3^- group having a larger trans effect than the Cl^- group [48].

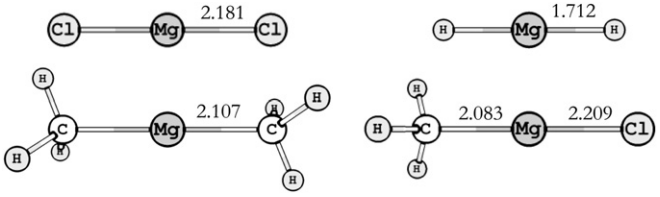

Fig. 1. Geometries (in Å, deg.) of our organomagnesium compounds, computed at BP86/TZ2P.

The gas-phase Gibbs energy difference associated with the Schlenk equilibrium [8]:

$$2CH_3MgCl \rightleftarrows Mg(CH_3)_2 + MgCl_2 \quad (4)$$

is 5.1 kcal/mol at the BP86/TZ2P level, which is not far from the 5.7 kcal/mol obtained at the MP4SDTQ/6-31G(d)//RHF/6-31G(d) including thermal corrections at the RHF/6-31G(d) level [45].

Hirshfeld and Voronoi charges for the studied monomers are collected in Table 1. As can be seen the Hirshfeld charge on Mg is +0.511, +0.603, +0.614, and +0.653 a.u. along MgH_2, $Mg(CH_3)_2$, CH_3MgCl, and $MgCl_2$, respectively. The enlargement of the Mg positive charge when going from MgH_2 to $MgCl_2$ is expected from the increase in the electronegativity of the ligands. For comparison, the Hirshfeld charge on Li at the same level of theory (BP86/TZ2P) is +0.414, +0.495, and +0.527 a.u. for LiH [18], $LiCH_3$ [15], and LiCl [19], respectively. While the Hirshfeld charges on the metal atom are similar for analogous organolithium and organomagnesium compounds, although somewhat higher for the latter, the negative charge on the ligands is halved in organomagnesium compounds. We showed for organolithium compounds that the component of the bond due to orbital interactions is quite important for understanding the bonding [15,17–19]. The trends observed in the charges provide an indication that the covalent interactions (HOMO–LUMO donation from ligand to metal ion) could be even more important in organomagnesium compounds than in their organolithium counterparts.

3.2. Tetramers

A previous theoretical study on the molecular structure of 51 isomers that can be constructed from the most stable $MgCl_2$ trimer by adding a new $MgCl_2$ to yield the $(MgCl_2)_4$ species concluded that the two most stable $MgCl_2$ tetramers are the D_{2h} and C_{2h}-symmetric forms **Iso_1A** and **Iso_1B** shown in Fig. 2 [13]. Apart from these two, we have also studied the T_d isomer **1** shown in Fig. 3 because the cube arrangement is the expected preferred structure in a purely ionic model and is the most stable tetramer in similar species such as $(NaCl)_4$ [49,50], $(KCl)_4$ [51], $(MgO)_4$ [50], or $(CpMgOEt)_4$ [52]. In addition, the cube arrangement is of interest for us because it allows direct comparison with a previous study on the tetramerization of MX (M = Li, Na, K, Rb; X = H, CH_3, F, Cl) species at the same level of theory [15,17–19]. The three isomers studied for all $(MgX_2)_4$ species (X = H, CH_3, Cl) are shown in Scheme 1. For the $(CH_3MgCl)_4$ species, we have optimized the three isomers only for the cases L_1 = Cl and L_2 = CH_3 in Scheme 1. The reason is the strong preference of 38 kcal/mol that we find for Cl, with respect to CH_3, to occupy bridge positions (cf. Refs. [45,53]). This preference can be attributed to more steric (Pauli) repulsion if, instead of chlorine atoms, the more bulky methyl groups enter the cubic core. This shows up as more Pauli repulsion and deformation energy ΔE_{def} (compare values of **4** and **6** in Table 1).

Tables 1 and 2 gather the gas-phase reaction enthalpy and Gibbs energy, as well as the electronic energy corrected for solvation in THF solution of the tetramerization process:

$$4L_1MgL_2 \rightarrow (L_1MgL_2)_4 \quad (5)$$

for the different $(L_1MgL_2)_4$ isomers. To our knowledge, there is no experimental data for the tetramerization energies of these species.

Table 1
Analysis of structure and monomer–monomer bonding in L_1–Mg–L_2 tetramers.[a]

	1	**2**	**3**	**4**	**5**	**6**
	Mg_4Cl_8	Mg_4H_8	$Mg_4(CH_3)_8$	$(ClMg)_4(CH_3)_4$	$(ClMg)_4(CH_3)_4$_stg	$(CH_3Mg)_4Cl_4$
Distances (in Å)						
Mg–Mg	3.544	3.044	2.984	3.624	3.621	2.960
Mg–L_1	2.494	1.994	2.363	2.531	2.531	2.345
Mg–L_2	2.183	1.700	2.100	2.082	2.082	2.210
L_1–L_1	3.511	2.552	3.637	3.535	3.537	3.610
Decomposition of tetramerization energy (in kcal/mol)						
ΔE_{Pauli}	218.6 (86.4)[b]	294.9 (133.2)[c]	352.0	223.2	223.0	379.1
ΔV_{elstat}	−225.8 (−187.1)[b]	−245.1 (−177.6)[c]	−317.3	−242.9	−242.8	−320.0
ΔE_{oi}	−161.3 (−41.7)[b]	−193.7 (−71.4)[c]	−191.0	−137.7	−137.8	−232.2
ΔE_{int}	−168.5 (−142.4)[b]	−143.9 (−115.8)[c]	−156.4	−157.4	−157.6	−173.1
ΔE_{def}	73.4 (16.3)[b]	51.4 (18.8)[c]	102.3	67.8	67.6	115.9
ΔE[d]	−95.1 (−126.1)[b]	−92.6 (−97.0)[c]	−54.1	−89.6	−90.0	−57.2
	58% EI (82%)[b]	56% EI (71%)[c]	62% EI	64% EI	64% EI	58% EI
	42% OI (18%)[b]	44% OI (29%)[c]	38% OI	36% OI	36% OI	42% OI
Thermochemical quantities						
ΔH_{298}	−92.8	−87.2	−50.9	−86.4	−86.7	−53.1
ΔG_{298}	−61.2	−57.9	−15.2	−56.1	−54.9	−18.3
ΔE (THF)[e]	−71.2	−75.3	−41.4	−62.3	−57.9	−46.4
Atomic charges (in a.u.) for monomer in equilibrium geometry[f]						
Q (Mg)	0.653 (0.706)	0.511 (0.568)	0.603 (0.507)	0.614 (0.579)	0.614 (0.579)	0.614 (0.579)
Q (L_1)	−0.326 (−0.353)	−0.256 (−0.284)	−0.302 (−0.250)	−0.358 (−0.378)	−0.358 (−0.378)	−0.256 (−0.202)
Q (L_2)	−0.326 (−0.353)	−0.256 (−0.284)	−0.302 (−0.250)	−0.256 (−0.202)	−0.256 (−0.202)	−0.358 (−0.378)
Atomic charges (in a.u.), dipole moment (in D) for monomer in tetramer geometry[f]						
Q (Mg)	0.414 (0.458)	0.405 (0.386)	0.423 (0.320)	0.412 (0.399)	0.411 (0.392)	0.428 (0.354)
Q (L_1)	−0.328 (−0.348)	−0.244 (−0.279)	−0.311 (−0.304)	−0.286 (−0.237)	−0.285 (−0.233)	−0.339 (−0.386)
Q (L_2)	−0.086 (−0.111)	−0.161 (−0.107)	−0.112 (−0.014)	−0.126 (−0.162)	−0.126 (−0.159)	−0.088 (0.032)
μ[b]	5.382	3.089	2.978	5.552	5.555	3.585

[a] All referred compounds are gas-phase local minima computed at BP86/TZ2P. See Fig. 3 for structures.
[b] In parenthesis values corresponding to the tetramerization process 4NaCl → $(NaCl)_4$ in T_d symmetry. From Ref. [19].
[c] In parenthesis values corresponding to the tetramerization process 4NaH → $(NaH)_4$ in T_d symmetry. From Ref. [18].
[d] EI = $[\Delta V_{elstat}/(\Delta V_{elstat} + \Delta E_{oi})] \times 100\%$; OI = $[\Delta E_{oi}/(\Delta V_{elstat} + \Delta E_{oi})] \times 100\%$.
[e] Tetramerization energy in THF solution.
[f] Hirshfeld charges (in parentheses: VDD charges).

The available theoretical data is also scarce and confined to a few values for the tetramerization energies of $MgCl_2$ [14] and MgH_2 [54]. As can be seen in Tables 1 and 2, in all cases, the tetramerization is favorable as expected from the well-known tendency of Grignard reagents and related organomagnesium compounds to form aggregates [10]. Magnesium dichloride has the largest (most stabilizing) tetramerization energy. This is in line with the expectation that the higher the polarity of the species, the larger the propensity to form aggregates. It is also consistent with the more favorable dimerization energy of $MgCl_2$ than that of $Mg(CH_3)_2$ [47].

Interestingly, the next most stable tetramer is that of MgH_2 although this is the least polar monomer. These trends for the T_d isomers are analyzed in detail through an energy decomposition analysis (EDA, see below). The most stable isomer for the $MgCl_2$ tetramer is the **Iso_1A** with D_{2h} symmetry. In terms of Gibbs energy, this isomer is 1.8 kcal/mol more stable than the **Iso_1B** with C_{2h} symmetry and this in turn is 13.3 kcal/mol more stable than the T_d form **1**. Similar energy differences (1.8 kcal/mol and 15.0 kcal/mol, respectively) were reported by Ahlrichs and coworkers using the HF/ECP method [14]. The **Iso_1A** and **Iso_1B** species are almost isoenergetic, and in fact when including solvent effects, the **Iso_1B** form becomes marginally more stable. In fact, at the MP2/6-311G(d) level of theory, this **Iso_1B** isomer with C_{2h} symmetry is found to be the most stable tetramer by 3.2 kcal/mol with respect to **Iso_1A** [13]. Therefore, depending on the level of theory one finds **Iso_1A** or **Iso_1B** isomers as the most stable $MgCl_2$ tetramer. The conclusion is that these two isomers are essentially of similar stability. Note that they also have the same number of bridge (six) and terminal (two) chlorines, while for the less stable T_d arrangement the number of terminal chlorines is four. This is an indication that in these clusters chlorines are more stabilizing ligands in bridge than in terminal positions. Interestingly, the C_{2h} **Iso_1B** species represents a small fragment of the magnesium dichloride lattice which is of $CdCl_2$ type [55]. An **Iso_1B**-like molecular arrangement also corresponds to the structure determined by single-crystal X-ray diffraction of the tetrameric Grignard reagent $[C_2H_5Mg_2Cl_3(C_4H_8O)_3]_2$ [56]. For MgH_2, the three isomers are almost isoenergetic, the C_{2h} **Iso_2B** being slightly more stable in the gas-phase. For the D_{2h} $(MgH_2)_4$ species, Wang and Andrews reported a tetramerization energy of about 102 kcal/mol calculated at the B3LYP/6-311++G(3df,3dp) level [54]. For the $Mg(CH_3)_2$ species, the most stable tetramer structure is **Iso_3A** of C_i symmetry. However, this structure is a saddle point, not a minimum on the potential energy surface. Therefore, it is less relevant for the discussion of the molecular structure of the $Mg(CH_3)_2$ tetramer. On the other hand, the **Iso_3B** isomer is almost isoenergetic with the isomer with cubic T_d arrangement (**3**). Finally, for the CH_3MgCl Grignard compound, the lowest Gibbs energy isomer corresponds to the cubic tetramer **4**.

Interestingly, as pointed out already above, the $(CH_3MgCl)_4$ isomer **4** that has chlorines as a bridge between Mg atoms and terminal methyl groups, is about 38 kcal/mol more stable than isomer **6** having the methyl groups as bridges and terminal chlorines. This is in line with the fact that the CH_3MgCl dimer is more stable having two chlorine bridges and terminal methyls than the other way round [53]. Isomer **5** differs from **4** on the staggered positions of the methyl groups and it is marginally less stable. Finally, isomer **Iso_4A** of C_{2v} symmetry (see Fig. 2) is close in energy to **4**. However, it is a saddle point, not a minimum on the potential energy surface and, therefore, again less relevant for the discussion of the molecular structures of CH_3MgCl tetramers.

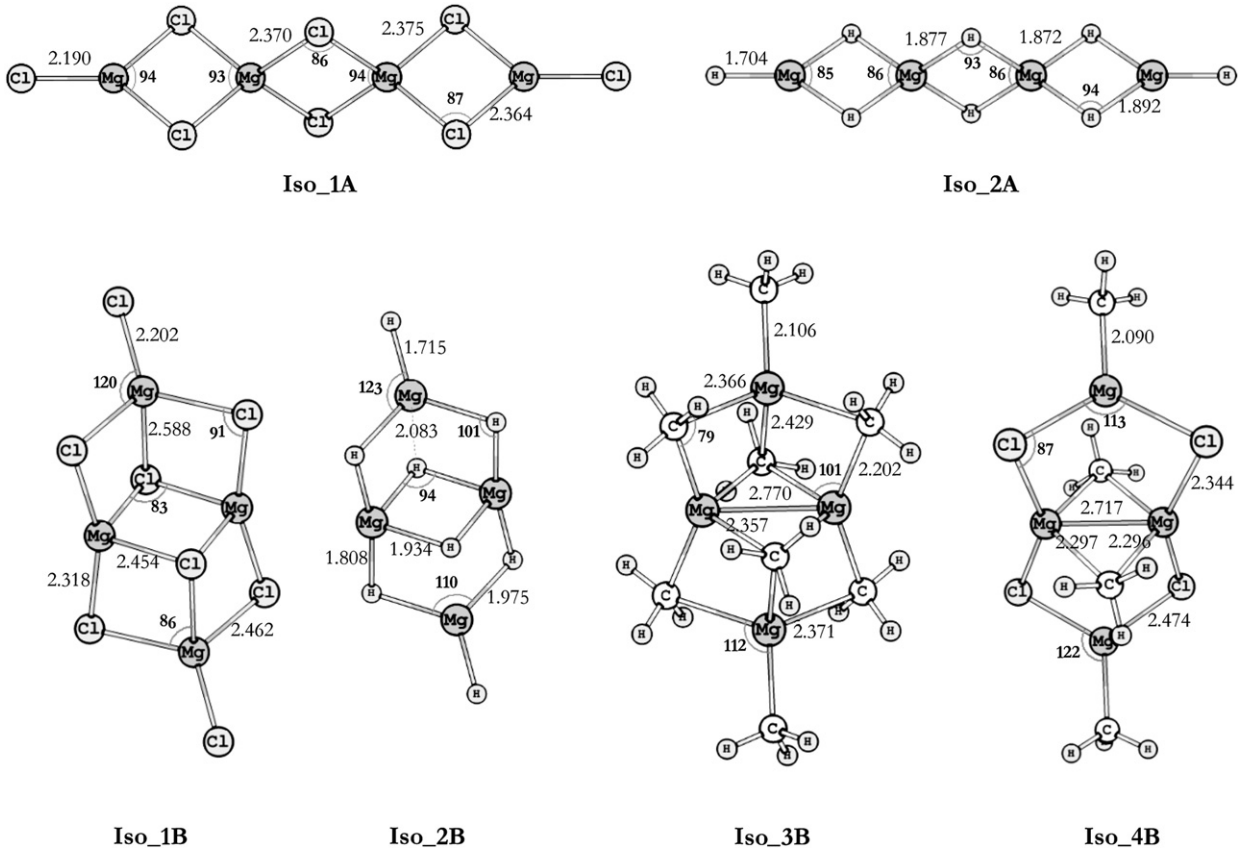

Fig. 2. Geometries (in Å, deg.) of isomeric low-energy tetramers $(L_1Mg)_4$–$(L_2)_4$ corresponding to equilibrium structures, computed at BP86/TZ2P.

When going from the monomers to the tetramers the Mg–Cl, Mg–H, and Mg–C bond lengths almost do not change for the substituents located at terminal positions, X_t, while for bridge substituents, X_b, the bond distances increase by 0.2–0.3 Å in most cases. At variance with T_d alkalimetal halides [19], the Cl–Cl distance between bridged chlorines in cube arrangements is slightly smaller than the Mg–Mg distance. This Mg–Mg distance is also larger than the H–H distance in the T_d MgH_2 tetramer but shorter than the C–C bond distance in $(Mg(CH_3)_2)_4$. Thus, the tetrahedral $(Mg)_4$ cage is larger than the $(R)_4$ cluster for R = H and Cl and smaller for R = CH_3. Finally, in solution the Mg–X_t bond lengths increase by 0.01–0.06 Å. This expansion is especially marked in the case of the most ionic Mg–Cl_t bond and less noticeable for the Mg–$(CH_3)_t$ bond. On the other hand, the Mg–X_b bond distances remain more or less the same in THF solution (see Figs. S2 and S3).

Next, we analyze the tetramerization energies of the T_d isomers using the EDA method. We have chosen the T_d isomer of the various monomers for two reasons: In the first place, the T_d structure is the energetically preferred isomer for the Grignard tetramer $(CH_3MgCl)_4$. Second, the analyses of T_d $(CH_3MgCl)_4$ can be directly compared to those of the corresponding T_d $(MgCl_2)_4$ and $(MgH_2)_4$ systems as well as to earlier analyses of the related T_d $(NaCl)_4$ and $(NaH)_4$ species. As can be seen in Table 1, the most stabilizing tetramerization energies for the cubic tetramers occur for $MgCl_2$ followed by MgH_2, CH_3MgCl, and $Mg(CH_3)_2$ that have tetramerization energies of −95.1, −92.6, −89.6 and −54.1 kcal/mol, respectively. The tetramerization energy of the latter is about 40 kcal/mol less stabilizing than that of the former systems. The decomposition of this tetramerization energy reveals that the electrostatic attraction ΔV_{elstat} is the dominant bonding force. Note that the most stabilizing ΔV_{elstat} term is found for the $Mg(CH_3)_2$ tetramer **3**, which consists of the deformed $(CH_3)_t$–Mg–$(CH_3)_b$ monomers with the smallest dipole moment (see Table 1; t = terminal; b = bridging). This is associated with the relatively short Mg–C_b bonds which are ascribed to favorable donor–acceptor orbital interactions that are possible between the carbanion-like methyl moiety of one monomer (the C_b–Mg σ bond orbital has much CH_3^- lone-pair character) with the magnesium ion of a neighboring monomer (the $C_{b/t}$–Mg σ^* acceptor orbital has much Mg^{2+} 3s character). This is also reflected by the favorably high orbital interactions whenever methyl moieties participate on bridge positions in the cubic core (see Table 1). For the same reason and also because steric hindrance caused by the bulkier methyl group, the $Mg(CH_3)_2$ tetramer is the one having the largest Pauli repulsion term and has a highly stabilizing ΔE_{oi} term. In addition, the $Mg(CH_3)_2$ tetramer has the largest deformation energy as could be expected from the fact that it is the species with the smaller $\angle L_1MgL_2$. The main difference between tetramerization energies of MgH_2 and $Mg(CH_3)_2$ comes from the deformation term that it is much larger in the cubic dimethylmagnesium tetramer. This makes the tetramerization process in MgH_2 especially favorable. Note that the bonding situation in **4** and **5** with bridge chlorines resembles that of $(MgCl_2)_4$, while that of **6** with bridge methyl groups is closer to that found in $(Mg(CH_3)_2)_4$.

The orbital interactions ΔE_{oi} between the L_1MgL_2 monomers are somewhat less stabilizing than the electrostatic attraction ΔV_{elstat} (see Table 1). Note however that ΔE_{oi} is far from being negligible with values between −193.7 and −137.7 kcal/mol: this corresponds to 36–44% of all bonding interactions, *i.e.*, ΔE_{oi} + ΔV_{elstat}. These orbital interactions are mainly provided by donor–acceptor interactions of occupied σ_{Mg-L_1} and L_1 lone pairs (if any) with the

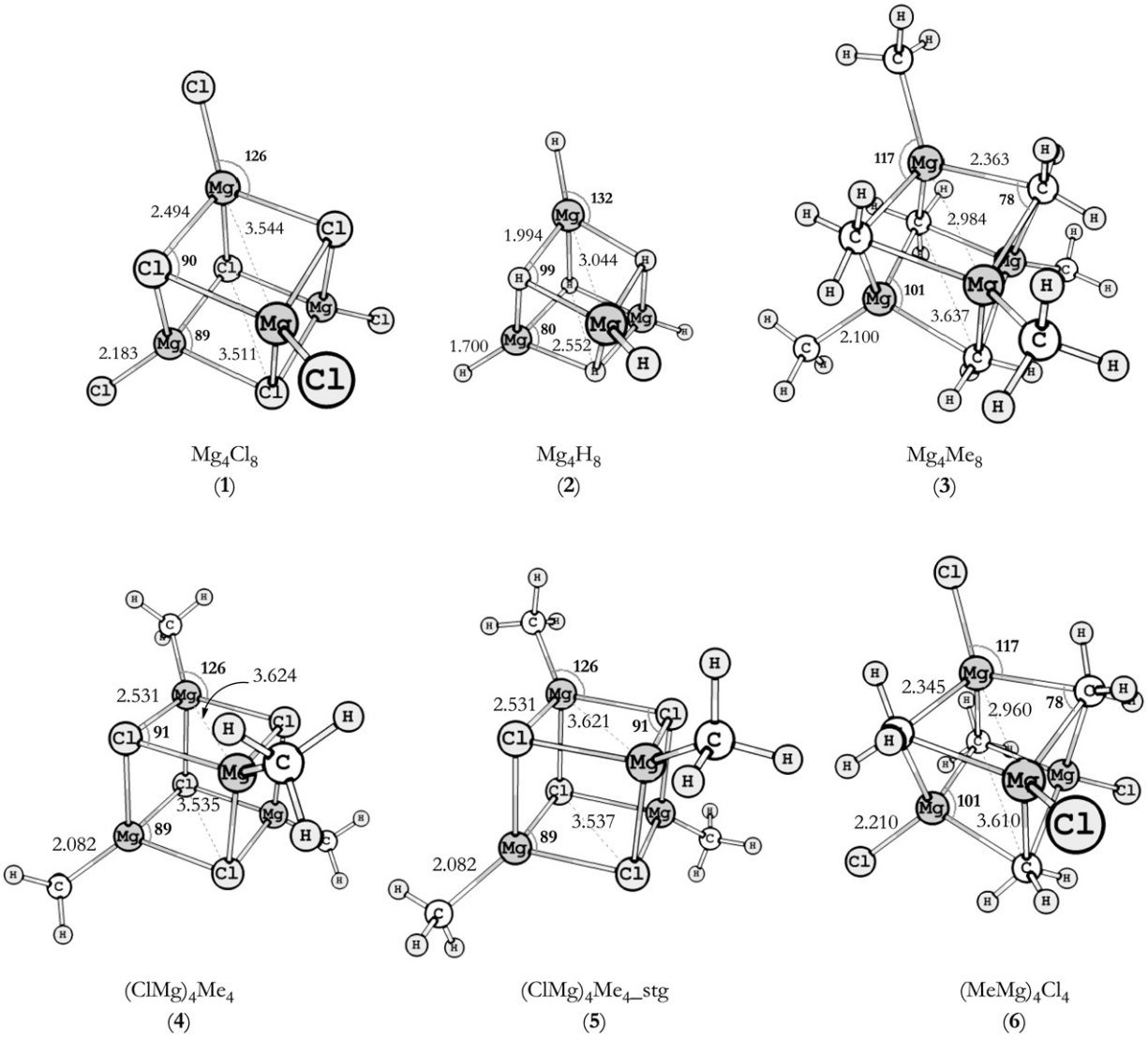

Fig. 3. Geometries (in Å, deg.) of organomagnesium T_d tetramers, computed at BP86/TZ2P.

unoccupied $\sigma^*_{Mg-L_1}$ (mainly located on Mg) of the monomers. Consequently, tetramerization reduces the charge separation because it favors the charge transfer from X to Mg as can be seen in Table 1 by comparing the charges on the different atoms in the isolated and deformed fragments and in the tetramer. In the latter, the charge on Mg is usually reduced by 0.1–0.2 a.u. A similar phenomenon was observed for alkalimetal hydrides, fluorides, chlorides and methylalkalimetals [15,17–19].

Finally, we compare the tetramerization of $MgCl_2$ and MgH_2 with that of the corresponding NaCl and NaH counterparts. The alkalimetal hydrides and chlorides appear to have a more stabilizing tetramerization energy than their magnesium counterparts. The bond analyses show that this originates from less steric congestion, as reflected by less Pauli repulsion and less deformation energy, in the case of the mono-coordinated sodium monomers than in the case of the di-coordinated magnesium monomers.

Table 2
Symmetry and tetramerization energies (in kcal/mol) of isomeric low-energy stationary points $(L_1Mg)_4$–$(L_2)_4$.[a]

	Iso_1A	**Iso_1B**	**Iso_2A**	**Iso_2B**	**Iso_3A**	**Iso_3B**	**Iso_4A**	**Iso_4B**
	Mg_4Cl_8	Mg_4Cl_8	Mg_4H_8	Mg_4H_8	Mg_4Me_8	Mg_4Me_8	$Mg_4Cl_4Me_4$	$Mg_4Cl_4Me_4$
Symmetry	D_{2h}	C_{2h}	D_{2h}	C_{2h}	C_i	C_1	C_{2v}	C_i
NIMAG[b]	0	0	0	0	3[c]	0	2[c]	0
ΔH_{298}	−109.5	−106.5	−84.6	−89.7	−59.1	−52.6	−87.9	−78.72
ΔG_{298}	−76.4	−74.5	−58.1	−60.6	−23.9	−16.0	−54.2	−46.6
ΔE (THF)[d]	−80.7	−81.2	−73.8	−82.5	−51.3	−46.6	−63.2	−57.7

[a] Computed at BP86/TZ2P. See Scheme 1 and Fig. 2 for structures.
[b] Number of imaginary frequencies.
[c] Low imaginary frequencies (**Iso_3A**: *i*12, *i*43, *i*45 cm^{-1}; **Iso_4A**: *i*32, *i*32 cm^{-1}) correspond to nearly-free methyl-group rotation.
[d] Tetramerization energy in THF solution.

Furthermore, although the electrostatic attraction ΔV_{elstat} is less stabilizing in the case of the sodium hydride and chloride tetramers than in the magnesium systems, its relative contribution to all stabilizing interactions $\Delta V_{elstat} + \Delta E_{oi}$ is larger.

4. Conclusions

The most stable isomer of methylmagnesium chloride tetramers, $(CH_3MgCl)_4$, is a T_d-symmetric cluster with a cubic $(MgCl)_4$ core and terminal CH_3 groups on the magnesium vertices, with the C_{2h} isomer being not far in energy. The isomer with methyl groups in an inner $(CH_3Mg)_4$ core is disfavored by some 38 kcal/mol, despite favorable orbital and electrostatic interactions, because of more steric congestion (showing up as more Pauli repulsion and more deformation energy between monomers in the tetramer). This follows from our computational analyses of the structure and bonding of a series of archetypal organomagnesium compounds, namely, the monomers and tetramers of the Grignard reagent CH_3MgCl as well as those of the MgX_2 (X = H, Cl, and CH_3) species at the BP86/TZ2P level of theory. We have also found that chlorine ligands are more stabilizing in bridge rather than in terminal positions for the most stable $MgCl_2$ tetramer structures.

Tetramerization energies of the T_d-symmetry structures of $MgCl_2$, MgH_2, CH_3MgCl, and $Mg(CH_3)_2$ are found to be −95.1, −92.6, −89.6 and −54.1 kcal/mol, respectively. Our bonding analyses of these tetramerization energies show that electrostatic attraction makes up 60% of all bonding terms in the tetramerization energy. HOMO–LUMO orbital interactions are responsible for the remaining 40%. This situation is similar to that found earlier for the corresponding organoalkalimetal clusters [15–19]. The aggregation energies of the organomagnesium monomers are however less stabilizing because the presence of two ligands (*e.g.*, CH_3MgCl) leads to more steric congestion as compared to only one ligand in the organoalkalimetal systems (*e.g.*, CH_3Li and CH_3Na).

Acknowledgments

We thank the following organizations for financial support: the HPC-Europa program of the European Union, the Netherlands Organization for Scientific Research (NWO), the Ministerio de Ciencia e Innovación (MICINN, project number CTQ2008-03077/BQU), the DIUE of the Generalitat de Catalunya (project number 2009SGR637), and the National Research School Combination-Catalysis (NRSC-C). Excellent service by the Stichting Academisch Rekencentrum Amsterdam (SARA), the Barcelona Supercomputing Center – Centro Nacional de Supercomputación (BSC–CNS), and the Centre de Supercomputació de Catalunya (CESCA) is gratefully acknowledged. Support for the research of M.S. was received through the ICREA Academia 2009 prize for excellence in research funded by the DIUE of the Generalitat de Catalunya. JOCJH gratefully acknowledge the Carl Trygger Foundation for support through CTS-09:144 postdoctoral fellowship.

Appendix. Supplementary material

Supplementary data associated with this article can be found, in the online version, at doi:10.1016/j.jorganchem.2011.06.014.

References

[1] E. Frankland, Q. J. Chem. Soc. 2 (1850) 263–296.
[2] (a) V. Grignard, Compt. Rend. Acad. Sci. Paris 130 (1900) 1322–1324;
(b) V. Grignard, Ann. Chim. 24 (1901) 433–490.
[3] F. Bickelhaupt, Chem. Soc. Rev. 28 (1999) 17–23.
[4] (a) H.G. Richey Jr., Grignard Reagents: New Developments, Wiley, Chichester, 2000;
(b) Z. Rappaport, L. Marek (Eds.), The Chemistry of Organomagnesium Compounds, Wiley-VCH, Weinheim, 2008;
(c) P. Knochel, W. Dohle, N. Gommermann, F.F. Kneisel, F. Kopp, T. Korn, I. Sapountzis, V.A. Vu, Angew. Chem. Int. Ed. 42 (2003) 4302–4320;
(d) J. Terao, N. Kambe, Acc. Chem. Res. 41 (2008) 1545–1554;
(e) A.C. Frisch, M. Beller, Angew. Chem. Int. Ed. 445 (2005) 674–688.
[5] D. Seyferth, Organometallics 28 (2009) 1598–1605.
[6] F. Bickelhaupt, in: H.G. Richey Jr. (Ed.), Grignard Reagents: New Developments, John Wiley & Sons, New York, 2000, pp. 299–327.
[7] F. Bickelhaupt, in: H.G. Richey Jr. (Ed.), Grignard Reagents: New Developments, John Wiley & Sons, New York, 2000, pp. 367–393.
[8] W. Schlenk, W. Schlenk Jr., Chem. Ber. 62 (1929) 920–924.
[9] (a) M. Linnolahti, T.A. Pakkanen, J. Phys. Chem. B 110 (2006) 4675–4678;
(b) T.N.P. Luhtanen, M. Linnolahti, T.A. Pakkanen, Inorg. Chem. 43 (2004) 4482–4486.
[10] M.A.G.M. Tinga, G. Schat, O.S. Akkerman, F. Bickelhaupt, E. Horn, H. Kooijman, W.J.J. Smeets, A.L. Spek, J. Am. Chem. Soc. 115 (1993) 2808–2817.
[11] K.J. Donald, R. Hoffmann, J. Am. Chem. Soc. 128 (2006) 11236–11249.
[12] M. Hargittai, Acc. Chem. Res. 42 (2009) 453–462.
[13] T.N.P. Luhtanen, M. Linnolahti, A. Laine, T.A. Pakkanen, J. Phys. Chem. B 108 (2004) 3989–3995.
[14] K. Eichkorn, U. Schneider, R. Ahlrichs, J. Chem. Phys. 102 (1995) 7557–7563.
[15] F.M. Bickelhaupt, M. Solà, C. Fonseca Guerra, J. Chem. Theory Comput. 2 (2006) 965–980.
[16] E. Matito, J. Poater, F.M. Bickelhaupt, M. Solà, J. Phys. Chem. B 110 (2006) 7189–7198.
[17] F.M. Bickelhaupt, M. Solà, C. Fonseca Guerra, J. Comput. Chem. 28 (2007) 238–250.
[18] F.M. Bickelhaupt, M. Solà, C. Fonseca Guerra, Faraday Discuss. 135 (2007) 451–468.
[19] F.M. Bickelhaupt, M. Solà, C. Fonseca Guerra, Inorg. Chem. 46 (2007) 5411–5418.
[20] M. Hargittai, P. Schwerdtfeger, B. Réffy, R. Brown, Chem. Eur. J. 9 (2003) 327–333.
[21] L. Schlapbach, A. Züttel, Nature 414 (2001) 353–358.
[22] E.J. Baerends, J. Autschbach, A. Bérces, F.M. Bickelhaupt, C. Bo, P.L. de Boeij, P.M. Boerrigter, L. Cavallo, D.P. Chong, L. Deng, R.M. Dickson, D.E. Ellis, L. Fan, T.H. Fischer, C. Fonseca Guerra, S.J.A. van Gisbergen, J.A. Groeneveld, O.V. Gritsenko, M. Grüning, F.E. Harris, P. van den Hoek, C.R. Jacob, H. Jacobsen, L. Jensen, G. van Kessel, F. Kootstra, E. van Lenthe, D.A. McCormack, A. Michalak, J. Neugebauer, V.P. Osinga, S. Patchkovskii, P.H.T. Philipsen, D. Post, C.C. Pye, W. Ravenek, P. Ros, P.R.T. Schipper, G. Schreckenbach, J.G. Snijders, M. Solà, M. Swart, D. Swerhone, G. te Velde, P. Vernooijs, L. Versluis, L. Visscher, O. Visser, F. Wang, T.A. Wesolowski, E. van Wezenbeek, G. Wiesenekker, S.K. Wolff, T.K. Woo, A.L. Yakovlev, T. Ziegler, Amsterdam Density Functional (ADF), Amsterdam (2006).
[23] G. te Velde, F.M. Bickelhaupt, E.J. Baerends, C. Fonseca Guerra, S.J.A. van Gisbergen, J.G. Snijders, T. Ziegler, J. Comput. Chem. 22 (2001) 931–967.
[24] J.G. Snijders, E.J. Baerends, P. Vernooijs, At. Nucl. Data Tables 26 (1981) 483–509.
[25] M. Swart, J.G. Snijders, Theor. Chem. Acc. 110 (2003) 34–41.
[26] E.J. Baerends, D.E. Ellis, P. Ros, Chem. Phys. 2 (1973) 41–51.
[27] S.H. Vosko, L. Wilk, M. Nusair, Can. J. Phys. 58 (1980) 1200–1211.
[28] A.D. Becke, Phys. Rev. A 38 (1988) 3098–3100.
[29] J.P. Perdew, Phys. Rev. B 33 (1986) 8822–8824.
[30] L. Seijo, Z. Barandiarán, S. Huzinaga, J. Chem. Phys. 94 (1991) 3762–3773.
[31] F.M. Bickelhaupt, N.J.R. van Eikema Hommes, C. Fonseca Guerra, E.J. Baerends, Organometallics 15 (1996) 2923–2931.
[32] P. Atkins, J. De Paula, Physical Chemistry. Oxford University Press, Oxford, 2006.
[33] (a) A. Klamt, G. Schüürmann, J. Chem. Soc. Perkin Trans. 2 (1993) 799–805;
(b) C.C. Pye, T. Ziegler, Theor. Chem. Acc. 101 (1999) 396–408.
[34] G.T. Velde, E.J. Baerends, J. Comput. Phys. 99 (1992) 84–98.
[35] F.L. Hirshfeld, Theor. Chim. Acta 44 (1977) 129–138.
[36] (a) F.M. Bickelhaupt, E.J. Baerends, in: K.B. Lipkowitz, D.B. Boyd (Eds.), Reviews in Computational Chemistry, vol. 15, Wiley-VCH, New York, 2000, pp. 1–86;
(b) K. Morokuma, Acc. Chem. Res. 10 (1977) 294–300;
(c) K. Kitaura, K. Morokuma, Int. J. Quantum Chem. 10 (1976) 325–340;
(d) T. Ziegler, A. Rauk, Theor. Chim. Acta 46 (1977) 1–10;
(e) T. Ziegler, A. Rauk, Inorg. Chem. 18 (1979) 1558–1565.
[37] (a) M. Hargittai, Chem. Rev. 100 (2000) 2233–2301;
(b) M. Hargittai, Struct. Chem. 16 (2005) 33–40.
[38] A. Shayesteh, D.R.T. Appadoo, I. Gordon, P.F. Bernath, J. Chem. Phys. 119 (2003) 7785–7788.
[39] H. Li, R.J. Le Roy, J. Phys. Chem. A 111 (2007) 6248–6255.
[40] J. Molnár, C.J. Marsden, M. Hargittai, J. Phys. Chem. 99 (1995) 9062–9071.
[41] V.V. Kasparov, Y.S. Ezhov, N.G. Rambidi, J. Struct. Chem. 20 (1979) 217–223 (Engl. Trans.).
[42] (a) E. Weiss, J. Organomet. Chem. 2 (1964) 314–321;
(b) E. Weiss, J. Organomet. Chem. 4 (1965) 101–108.
[43] E.C. Ashby, L. Fernholt, A. Haaland, R. Seip, R.S. Smith, Acta Chem. Scand. A 34 (1980) 213–217.
[44] M. Hogenbirk, G. Schat, O.S. Akkerman, F. Bickelhaupt, W.J.J. Smeets, A.L. Spek, J. Am. Chem. Soc. 114 (1992) 7302–7303.
[45] J. Axten, J. Troy, P. Jiang, M. Trachtman, C.W. Bock, Struct. Chem. 5 (1994) 99–108.

[46] J. Axten, M. Trachtman, C.W. Bock, J. Phys. Chem. 98 (1994) 7823–7831.
[47] A.W. Ehlers, G.P.M. van Klink, M.J. van Eis, F. Bickelhaupt, P.H.J. Nederkoorn, K. Lammertsma, J. Mol. Model. 6 (2000) 186–194.
[48] F.R. Hartley, Chem. Soc. Rev. 2 (1973) 163–179.
[49] (a) A. Heidenreich, I. Oref, J. Jortner, J. Chem. Phys. 96 (1992) 7517–7523;
(b) A. Ayuela, J.M. López, J.A. Alonso, V. Luaña, Physica B 212 (1995) 329–342;
(c) S. Zhang, N. Chen, Physica B 325 (2003) 172–183.
[50] M.-J. Malliavin, C. Coudray, J. Chem. Phys. 106 (1997) 2323–2330.
[51] (a) A. Aguado, A. Ayuela, J.M. López, J.A. Alonso, Phys. Rev. B 56 (1997) 15353–15360;
(b) J.P. Rose, R.S. Berry, J. Chem. Phys. 96 (1992) 517–538.
[52] H. Lehmkuhl, K. Mehler, R. Benn, A. Rufińska, C. Krüger, Chem. Ber. 119 (1986) 1054–1069.
[53] S. Yamazaki, S. Yamabe, J. Org. Chem. 67 (2002) 9346–9353.
[54] X. Wang, L. Andrews, J. Phys. Chem. A 108 (2004) 11511–11520.
[55] I.W. Bassi, F. Polato, M. Calcaterra, J.C.J. Bart, Z. Kristallogr. 159 (1982) 297–302.
[56] J. Toney, G.D. Stucky, J. Organomet. Chem. 28 (1971) 5–20.